Bulletin of Earth Sciences of Thailand

Structural Style and Fracture Characteristics of Thrusted and Folded Permian Carbonates in the Siam City Cement Company Quarry, Tabkhwang, Saraburi Province, Central Thailand; Analogs for Fractured Carbonates

Suphawich Thanudamrong

Petroleum Geoscience Program, Department of Geology, Faculty of Science,
Chulalongkorn University, Bangkok 10330, Thailand

*Corresponding author email: suphawich.tha@gmail.com

Abstract

The Saraburi group Permian limestone is well exposed in the Siam City Cement quarry and is made up of a variety of limestone lithofacies, showing variable degrees of deformation and fracture intensity. It provides an excellent opportunity for the study of fracture character and its relation to structural style. Rock units were classified into six lithofacies, which are: thick bedded limestone, highly sheared cataclastic limestone / siliceous carbonate mudstone interbedded with shale, medium to thick bedded limestone, well-bedded limestone, shale with andesitic intrusives and dolomitic limestone. Six lithofacies were grouped and interpreted as equivalent to Phu Phe formation (Well-bedded limestone, shale with fine grained andesite), which is the oldest formation and Khao Khad formation (thick bedded limestone, siliceous carbonate shale and medium to thick bedded limestone) that is the youngest formation. The Phu Phe formation tectonically overlies the Khao Khad formation. Three thrust faults are present, trending approximately northwest-southeast with dips varying from 7^{o} – 64^{o} SW. Synforms and antiforms show Z asymmetrical folds, chevron folds, tight folds and similar (class 3) folds, all are present regionally and fault-propagation folds are associated with the main thrust. Three fracture sets are present, they are; longitudinal, transverse and oblique sets. The longitudinal (parallel to fold axis) set hosts the highest fracture density and is best developed in the areas close to the main fold hinges and intensity varies with distance to the fold and shows the highest density in thin-bedded limestones. Of the other two sets of fractures found in the area, the transverse set (perpendicular to fold axis) has a lesser density compared to the longitudinal set. The gamma log in all the measure limestone cores is consistently low, and the level of calcite veining (which was consistently seen to be composed of non-uraniferous vein calcite) did not sufficiently change the low background gamma signal to be visible in the log. The spectral gamma results of this study shows that a gamma log cannot be used to define zones of fracturing in a Permian carbonate host in Thailand. Stable oxygen and carbon isotope results show a consistently depleting trend that is at the higher temperature end of the marine carbonate normal burial trend. The two-plot fields (matrix and calcite veins) overlap indicates the ongoing recrystallisation of the matrix as the rocks were buried more deeply, fractured and deformed. The similarity of their plot fields also argues that most of the fluids precipitating as calcite veins were locally derived and not transported substantial distances as anomalous fault-fed fluids. The improved understanding of fracture characteristics and controls, related to the macroscopic structural geometry that comes from this work will contribute to the construction of better fracture reservoir models and their use in the optimal administration of fractured carbonate reservoirs in this region and elsewhere in SE Asia.

Keywords: Saraburi limestone, fracture orientation, fracture densities, stable isotope

1. Introduction

Fractures are recognized as an important factor in the exploration and production of hydrocarbons, and many major oil fields are classified as producing from fractured reservoir. Carbonate rocks that are host to oil and gas reservoir commonly have low matrix porosity and permeability. Fracture is related to the deformation area which is fold and thrust belt. The prediction of fracture orientation and fracture density in the subsurface is difficult because of the limitation of data availability. Cores and image log are limited to orientated the fracture orientation and understand the fracture density. The analogy or interpolation the data in subsurface is required proper analog model and high-quality data. The surface fracture characterization is an excellent tool to analog the fracture orientation, fracture density to the subsurface. To develop the proper surface fracture model, the fracture orientation, fracture densities have to be studied together with the structural styles and its relation to fractures. The Study area is located at Siam City cement company ltd quarry at Tab Khwang subdistrict, Kaeng Khoi district, Saraburi province. The study outcrop in the area is in an active cement manufacture quarry

This study aims to document the structural style, timing of structural events and understand the relationship of the deformation zone and fracture characteristics.

2. Methods

The field investigation involved systematic field transects, stratigraphic mapping and, particularly, measuring structural data from inactive quarries within the mine. At the outcrop scale, the structural data include bedding, cleavage, and the orientations of joint, fractures, folds, faults planes and sense of movement indicator as slickensides were collected. These data were used to document and build the understanding of geological framework within the study area. The lithology description involves macroscopic analyses that define rock types, fabrics, textures and obvious diagenetic features using the classification of Dunham (1962).

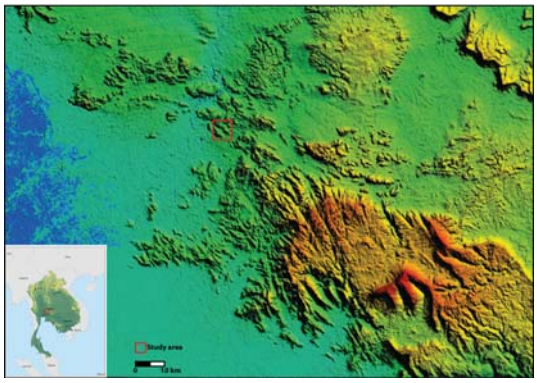

Figure 1. Location of the study area in Saraburi province, central of Thailand, and the base map is DEM30 (downloaded on 10 July, 2011)

Bedding orientation was used to define the structural position and its relation with to the regional structural framework. Fault, fractures orientation and fractures intensities were recorded at each location. The spectral gamma ray profiles were run on the selected cores data to create the link of surface to subsurface. The core fracture study was performed to analyze the fracture intensity with the relation to lithology, and fracture set without orientation. Nineteen representative samples were selected for thin section analysis of rock type, texture, and diagenetic evolution at the microscopic size by using a polarized light microscopic. Half of each thin section was stained with Alizarin red S and potassium ferricyanide in order to distinguish the mineralogies of the grain and cement by distinguishing the differential reaction to the chemical between calcite, ferron calcite and dolomite. The selected samples from representative samples were analyzed using XRD in order to support the types of minerals seen in the thin section. The

stable isotope analysis was run on selective samples to better define the origin and timing of both cement and matrix and its relation to the diagenetic and geological evolution within the study area.

3. Results

3.1. Structure

The regional strike of the rocks unit mostly lays in NW-SE direction and locally in east-west direction. Generally, the dips are moderate to the SW and S direction. In the field investigation, the successive stratigraphy was described based on the rock types of the unit at each outcrop location.

3.1.1) Lithofacies

Throughout the study area, there are six different lithofacies as follows; 1) Unit 1: Thick bed limestone, wackestone-packstone, rudstone, 2) Unit 2: Shale and silt medium to dark grey, sandstone thin bed with highly deformed, 3) Unit 3: Medium to thick bed mudstone, wackestone to packstone, rudstone, 4) Unit 4: Shear zone, thin to medium bedded packstone to grainstone, rudstone, 5) Unit 5: black shale with igneous intrusive, and 6) Unit 6: Massive limestone and dolomitic limestone.

The study area was divided into three subareas subarea is bounded by the surfaces of discontinuity between the successive of rock layers, the rock boundaries unit. In each subarea, the bedding plane orientations were recorded and analyzed by using the lower-hemisphere equal area stereonet plots.

Subarea 1 includes the lithofacies unit 4, 5 and 6. The bedding planes mostly strike NW-SE are inclined to the SWt direction with moderate to rather steep dip values. The minor folds as seen in this subarea were mostly gently plunging. Their axes are oriented NW-SE, which conforms to the strike of bedding planes. Subarea 2 includes the lithofacies unit 3 and 4. The bedding planes mostly trend NW-SE and E-W, and incline to the SW and south directions. The dip values vary from gentle to steep. Subarea 3 includes the lithofacies unit 1 and 2.

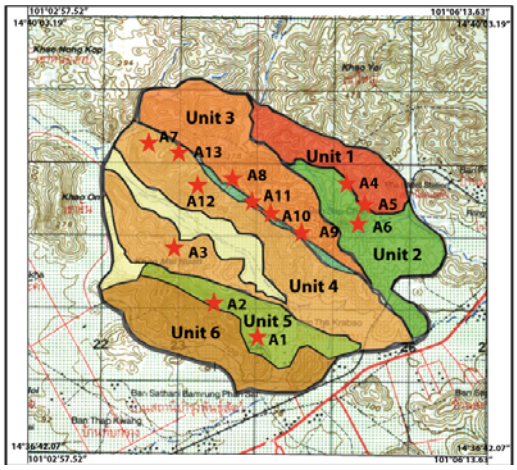

Figure 2. Illustrated the six lithofacies and the outcrop locations in the study area. This map should be used to locate all the filed photograps.

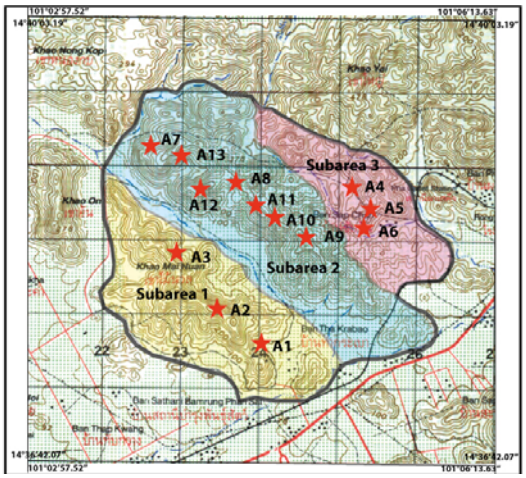

Figure 3. Illustrated the three subareas and the outcrop locations in the study area

Besides, the fault planes, minor fold elements, fracture orientation and other penetrative structures were similarly analyzed to contribute the information to define the relationship between structural styles and fracture characteristic.

3.1.2) Thrust fault

The high angle reverses fault and thrust faults are well exposed especially in the middle of the quarry and in the northeast zone above the thick bed. The thrust is marked by strong deformation zone including fault smear zone in shales, calcite filled veins, calcite veins parallel to the thrust and slickenside. There are three main thrust faults in sub-areas 1, 2 and 3. In subarea-1, the thrust trends approximately NW-SE, dips 26° to the SW and slickenside striations trend nearly NW-SE direction (Figure 4).

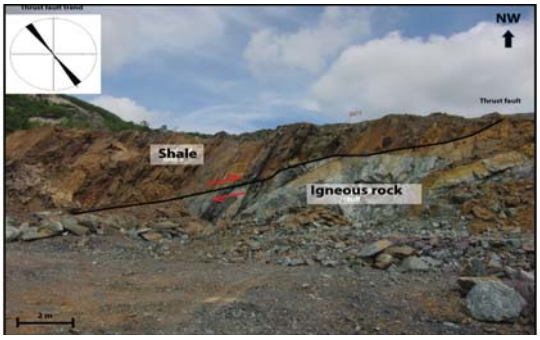

Figure 4. Photo of thrust fault at outcrop A1 in subarea 1

In sub-area-2, there are several outcrops, which show the thrust zone. The thrust plane is orients NW-SE, dips 45° - 64° to the southwest and the striations trend approximately NW-SE (Figure 5).

Figure 5. Photo of thrust fault and shear zone in the subarea-2 at outcrop A12. (A) Medium to thick bed limestone (unit 3), (B) Thin to medium bed limestone (unit 4)

In the sub-area-3, several thrust faults that form the main thrust fault zone, they strike WNW-ESE, and dip to SSW 7° - 55°. Striations in this area are trends NW-SE direction (Figure 6).

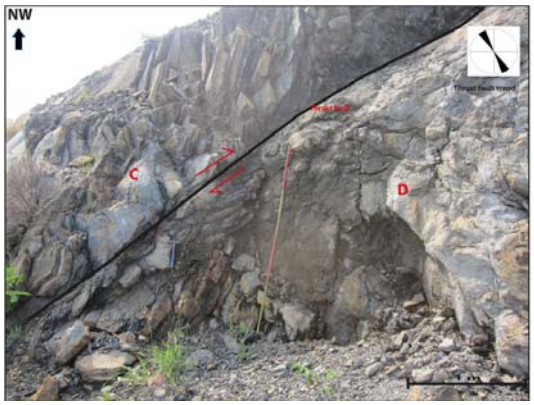

Figure 6. Photo of thrust fault at the subarea-3 at lower part of outcrop A5. (C) Shale (unit 2), (D) Thick bed limestone (unit 1)

The main thrust fault was observed along the boundary of thin to medium bed limestone and medium to thick bed limestone in sub-area-2 and oriented in NW-SE trend. The thrust plane was observed at several outcrops with the few meters width of shear zone. The minor two thrust faults were located in the subarea 1 and 3. At subarea-1, the thrust fault located in a Shale unit. There is no clearly evi dence to perform the stratigraphic succession investigation across the dolomitic limestone and black shale unit that lead to unable to identify the thrust in this section. However, we know the black shale is involved in a thrust zone because it is so highly deformed. At Subarea-2, the shale unit is thrusted over a thick limestone unit (Figure 7).

Regarding the lithofacies in the study area, the stratigraphy was interpreted into two formations. The younger formation consist of lithofacies unit 1 that equivalent to unit 3 and unit 2. This formation is relatively equivalent

to Khao Khad formation (Hinthong, 1985). The older formation comprise of unit 4 that interpreted as the lateral equivalent to unit 6 and unit 5, and it is equivalent to Phu Phe formation (Hinthong, 1985).

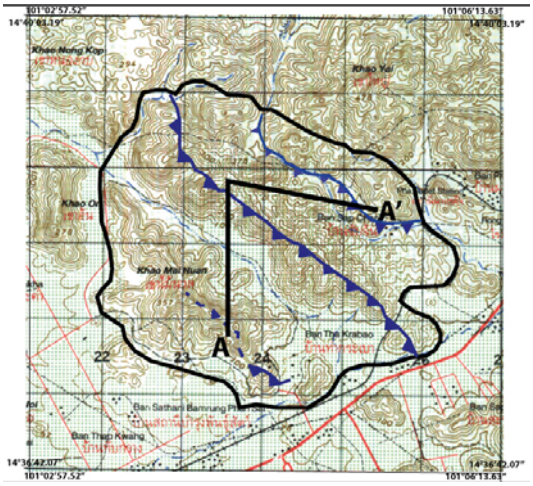

Figure 7. Map illustrating the interpreted main thrust fault and the minor thrust faults in the study area.

In addition, the structural field investigation indicated that the older formation is tectonically overlies on the younger formation. Therefore, the three thrust faults in the study area are interpreted as an imbricated thrust faults (Figure 8)

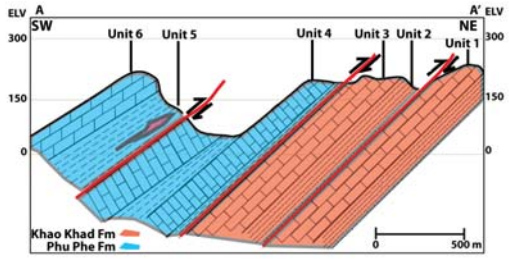

Figure 8. The interpretation of imbricated thrust faults across the study area in NE-SW.

3.1.3) Folds

In this study, several types of fold were. In subarea-1, the minor folds in the incline rock unit were composed of synforms and antiforms that showed Z asymmetrical folds, chevron folds, tight fold and similar (class 3) folds. The major axial surfaces of the folds are oriented approximately WNW - ESE, dip around 55^{o} -70^{o} to the southwest and plunge to the southeast. The different fold styles perhaps indicate the different folding mechanism and tectonic force system (Figure 9).

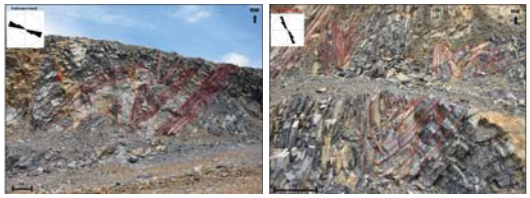

Figure 9. Photo of the folding in subarea 1 at outcrop A3 (left) Z type fold in thin to medium bed limestone, (right) tight fold, &chevron fold

In subarea-2, which is in the main thrust fault zone, the fault related folds were observed locally in limestone unit. The fault propagation folds is comprise majority of the fault related folds observed within the zone across the quarry from NE to SW. The folds formed during a propagation of the fault tip. The axial surface of the fault propagation fold is oriented approximately NW-SE, and dips around 45^{o} -64^{o} to the SW and plunges to the W (Figure 10). In subarea-3, the fault propagation fold was also observed as a major fault related fold.

Figure 10. Photo of fault propagation folds in out crop A7. (left) fault propagation fold (unit 4)

The undulating cross folds as seen from the variation of the bedding plane orientation recorded a different fold creating stress field from that creating the main folds and thrusts. There are at least two major areas cross folds are observed. The major fold axis of the undulating cross fold was measured and resulted in two significant directions, which are NW-SE and NE-SW. This fold axis perhaps resulted from the horizontal stress (sigma 1) in the NE/SW and NW/SE directions. These folds are culminations related to duplexes developed in the shale units (Figure 11).

Figure 11. Undulating cross fold in the shale unit at subarea 3.

3.1.4) Strike-Slip fault

A large strike slip fault trends approximately NW - SE and displays the left lateral sense of motion, dip angle is 65° northeast. The sinistral fault is offset by a NNW – SSE right lateral strike-slip fault, dip angle 84°east. This means the two faults are not related but represent different stress regimes. The dextral fault is later than the sinistral one that drated of strike-slip fault offset shows in figure 12.

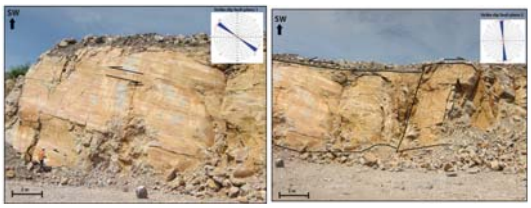

Figure 12. Photo of two offset strike-slip faults in subarea-2.

3.1.4) Strike-Slip fault

The orientation of the strata is rather uniformed, majority trends in northwest - southeast and locally east-west. The bed mostly dipping southwest and some local area observed the variation in bedding especially close to the fold and strongly deformation zone (Figure 14).

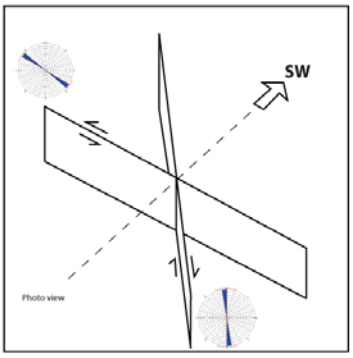

Figure 13. Illustrated the draft of two offset strike slip faults.

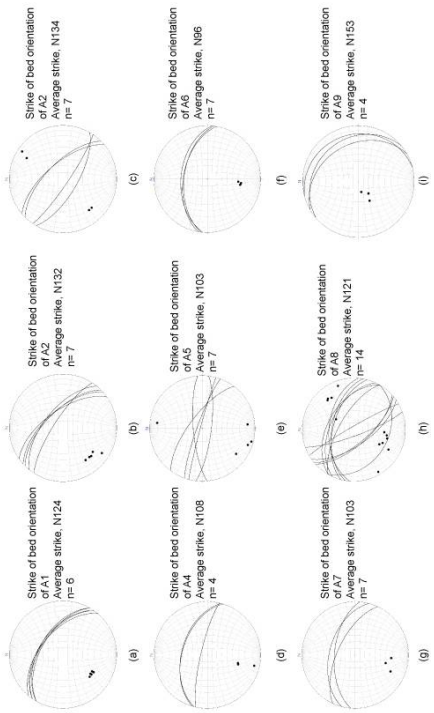

Figure 14. Stereonets showing the strikes of the bedding plane (a-b) bedding planes of the subarea-1, (c-f) bedding planes of the subarea-2, (g-i) bedding planes of the subarea-3

3.2. Fracture Analysis

3.2.1) Fracture orientation

Based on field investigation anf fracture plots, two catagories of fracture origins were observed; the tensional fractures which are sub-parallel to fold axis and sub-perpendicular to fold axis, and shear fracture which oriented conjugate. Fracture orientation data were restored by bedding rotated to horizontal which of the field observation present day fracture orientation can be related to original pre-deformation orientation, four main sets of fracture were identified. The two most dominant fracture sets are a longitudinal set, which is subparallel to the fold axis and normal to bedding plane, which have a mean strike of 138^{o} and dip of 83^{o} SW&NE, and a transverse set, which is perpendicular to the fold axis and bedding plane, with a mean strike of 59^{o} with dips 72^{o} SE and 74^{o} NW. Two other sets, one with a mean strike of 95^{o} and a 60^{o} N and another with a strike of 175^{o} and 70^{o} W. Several additional sets are present, but may just reflect to the complexity of the fracture orientation itself (Figure 35).

3.2.2) Fracture densities

For each fracture set, the distributions of fracture densities were analyzed and the fracture density of each set was defined as the summed number of all fractures of that set per unit. Four different representative outcrop locations were drawn the fractures orientations to perform the fracture density analysis (Figure 16). The densities of both longitudinal and transverse sets varied for the outcrop in the study area, with the longitudinal fractures exhibiting grater variability. This variation was attributed preliminary to the structural position, so the control of structural position on the fracture density was further analyzed.

3.2.2) Control of Structural Position on fracture density

Variations of fracture density with respect to the structural styles were studied on a number of structures. In general, the fracture densities are higher within strongly deformed zones such as on the hinge of fold and fault related fold than on the limb and the bed with distance from the deformation zone. Also, the thicker bed has higher density than the thinner bed as shown in outcrop A12. Furthermore, the longitudinal fracture sets show significant variation in density with distance from the nearest fold hinge. The transverse and oblique fractures, which are unrelated to the fold hinges, show little variation in fracture intensity with respect to distance from deformation zone.

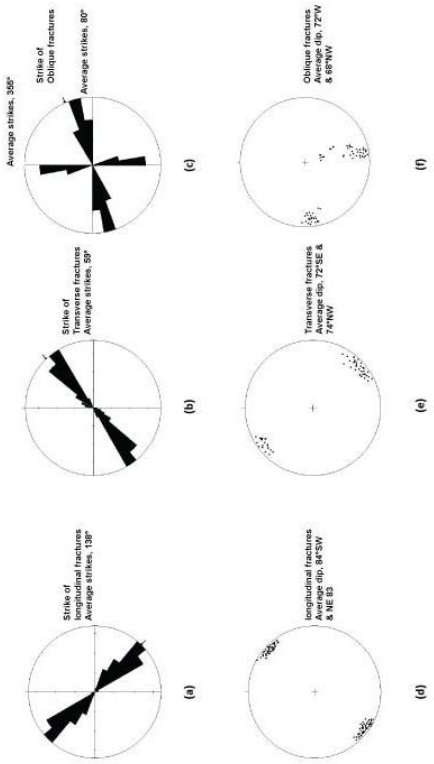

Figure 15. Rose diagram and stereographic plot poles to planes of the orientation of longitudinal, transverse and oblique fractures, with bedding rotated horizontal

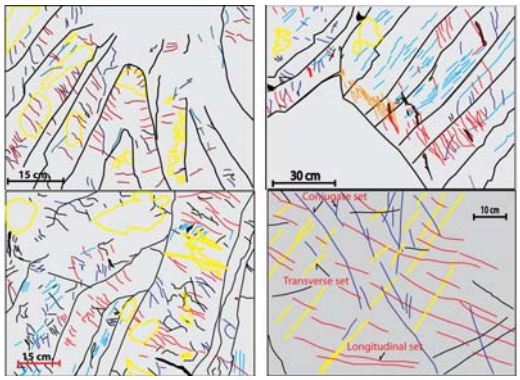

Figure 16. Illustration the draft of fracture sets from four selected outcrops (outcrop locations see figure 6). (upper left) fracture set at the fold in thin bedded limestone at out crop A3, (upper right) fracture set near the shear zone in thin bedded limestone at out crop A13, (lower left) fracture set at fault propagation fold in thin bedded limestone at out crop A12, (lower right) fracture set at the pavement limestone at out crop A5 shows clearly four fracture sets (red: fracture with orientations paralllel to fold axis, yellow: fracture with orientations sub-perpendicular to fold axis, blue: oblique fracture sets)

3.3 Spectral gamma ray and fracture density in core

Eight cores were measured and a three-point moving average was applied to smooth the spectral gamma profile and so make it more directly comparable with a wireline gamma collected from a petroleum well (Figure 17).

Regarding core spectral gamma ray investigation, the total gamma ray was recorded as relatively low in both limestone and shale lithofacies (although, as noted earlier what are called shales in some of the cores are perhaps better classified as siliceous cataclastic of intensely sheared carbonates).

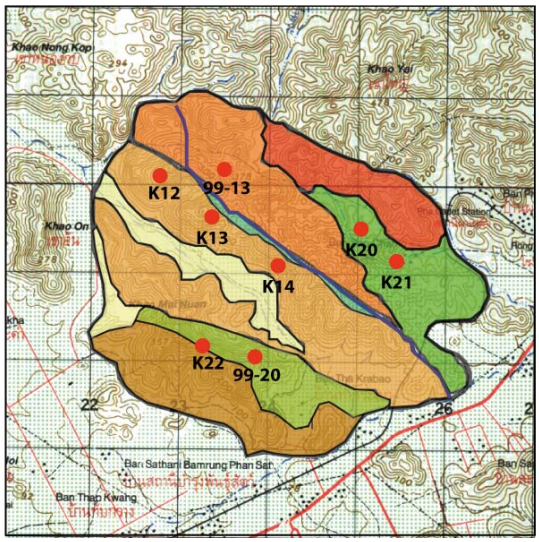

Figure 17. Illustrated of cores locations of spectral gamma ray measurement.

This could be explained by the presence of high SiO2 content and low K2O content in subarea-3 and resulted in low K values that could be interpreted as low clay content in shale lithofacies. Fracture density along the core is also related to the proximity to a deformation zone and lithology which in the past has been call shale is actually a zone of intenses deformation in the carbonate and can be tied back to zones of increased fracture intensity. This is confirmed by the surface investigation in the same area as the wells (Figure 18). At the start of this stage of the work it was felt that the uranium trace in these profiles would perhaps be related to the depositional profile in some parts of the cores, but that a high uranium curve could relate to a high fracture intensity zone (greater fluid mobility of uranium in such a zone).

The end result was that neither was true in the region. The gamma log in all the measure limestone cores was consistently low, and the level of calcite veining (which was consistently seen to be composed of non-uraniferous vein calcite) did not sufficiently change the low background gamma signal.

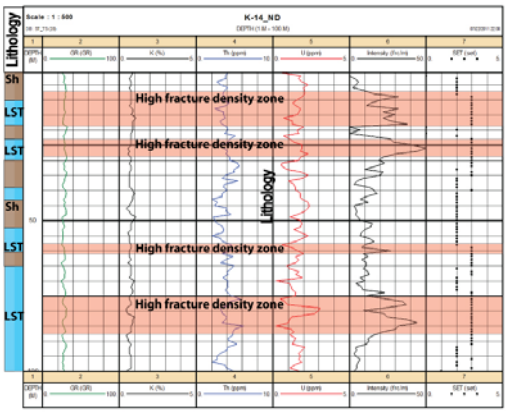

Figure 18. Spectral gamma ray profiles with fracture density of core well K-14

There was never enough variation away from low background levels to make a calcite-veining associated fracture/leach zone visible in a pseudogamma log. The spectral gamma results of this study were run in lithologies and deformation styles similar to what occurs in the subsurface of NE Thailand, where zones of potential fractured reservoirs occur, hosted in Permian carbonates. This work clearly shows that a gamma log cannot be used to define zones of fracturing in a Permian carbonate host. To put it simply, a gamma profile in the Permian carbonates of Thailand is a poor discriminant of rock type (it does not clearly define zones of wackstone versus rudstone in the studied cores), and it does not define zones of more intense deformation in a limestone (calcite veins and calcite-filled fractures associated with the deformation are not uraniferous).

3.4 Stable Isotope

Stable oxygen and carbon isotope results show a consistently depleting trend that is at the higher temperature end of the marine carbonate normal burial trend. The two-plot fields (matrix and calcite veins) overlap indicates the ongoing recrystallisation of the matrix as the rocks were buried more deeply, fractured and deformed. The similarity of their plot fields also argues that most of the fluids precipitating as calcite veins were locally derived and not transported substantial distances as anomalous fault-fed fluids.

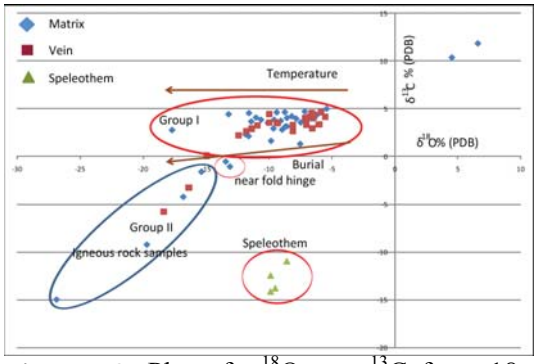

Figure 19. Plot of $\sigma^{18}O$ vs $\sigma^{13}C$ from 18 sample sites for carbonate matrix, calcite vein and speleothem

The trend of oxygen depletion in the carbonate matrix (right to left in the figure 19) demonstrates a similar increasing temperature trend to that seen in the calcite-filled veins they host. The two plot field (matrix and calcite veins) overlap indicating that there was ongoing recrystallisation of the matrix as the rocks were buried more deeply, fractured and deformed. The similarity of their plot fields also argues that most of the fluids precipitating as calcite veins were locally derived and not transported substantial distances as anomalous fault-fed fluids.

4. Discussion

4.1 Structural styles and its relation to fractures

The data from current study suggests that this major thrust fault is located in the study area, with a northwest - southeast trend and dipping to the southwest. The lithofacies of unit 4 end abruptly where they lie above unit 3. The abrupt boundary is also characterized by evidence of thrust faulting, such as shear zones, fault drags, slickensides and especially fault-related folds that are fault propagation folds. The idealized of imbricated thrust fault crossection shows in Figure 18.

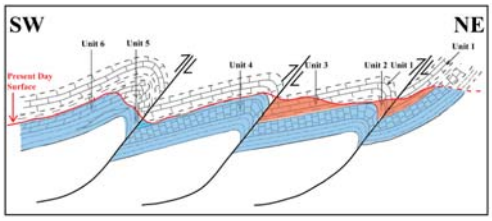

Figure 20. Idealized cross section of the study area.

Data from the typical strike and dips of the fault plane in this study indicate a NWSE direction and a horizontal principal (σ1) in a NW/SE direction (Figures 20 and 21).

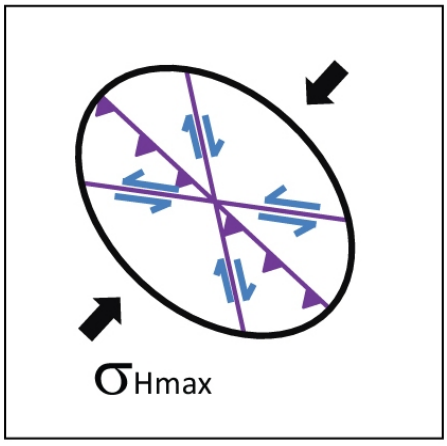

Figure 21. Generalized stain ellipse associated thrust fault in the study area

The systematic variation in fracture orientation and fracture density indicates that fracture orientation and fracture density are related to the major thrust fault and folding. However, cross cutting relationships for the described fracture sets do suggest some unclear fracture patterns exist. In the study area, a combination of thrust faults, conjugate strike-slip, and undulating cross folds suggest that the horizontal principal stress might be in more than one direction. Three types of fracture orientation, namely longitudinal, transverse and oblique, were observed in relation to the structural styles in the study area.

Sometime after the youngest age of the sedimentary rock, the area became the venue of strong thrusting movement(s) / folding. As the Indosinian orogeny is generally recorded in rocks in the region, the orogeny is the main key that controlled the structural deformation in the study area. In the study area, Permian sedimentary rocks were intensively folded to form the northwest-southeast trending and southwest dipping strata, thrusted in the ductile to brittle stages, while the undulating cross folding suggests that driving tectonic event had more than one phase. During the Mesozoic, other orogenic episodes occurred but they may not be significant in the study area. At the end of the Mesozoic Era, another orogenic episode occurred, that was Himalayan Orogeny and this could be the last tectonic event that effected to the study area.

4.2 Fracture characterization

The relationship of fracture orientation and fracture density to the fold and thrust system can be explained by the observation that during the early stage of concentric folding, the bedding was subjected to layer parallel extension, this resulted in the formation of longitudinal fractures. With continued folding, bending was concentrated along the hinge so that the fracture densities increased along the hinge. The transverse fractured perhaps are related to the change in curvature parallel to the fold axis and caused by variation in fold plunge. As well as in these fault-related thrusts, the fracture pattern was formed in a similar stage with a similar fracture pattern in a fault propagation fold. Fracture densities in the study area are also related to variations rock type (lithofacies). Thin bedded limestones tend to contain higher fracture densities than thick bedded limestones.

4.3 Application in fractured reservoir characterization

The fracture pattern studied in the outcrop may induce an understanding of fluid flow, which will analogue reliably into the

subsurface hydrocarbon reservoir. In particular, in the study area a widespread well-connected fracture system on the surface outcrop is related to the anticlinal folding. The faults are associated with narrower zones with high fracture intensity.

Typically, fractures in the study area are now filled or partly filled with carbonate cement, and their apertures have locally been enlarged (depressuring and meteoric solutioning) along the fracture plane. Such features will not be present in the subsurface and the large proportion of the fracture filled by carbonate cement formed during burial (as indicated isotopically) do not create favorable reservoir properties (in terms of fluid flow).

5. Conclusions

The Saraburi group Permian limestone in the study shows major thrust fault located in the center of the study area has a NW-SE trend and is SW dipping. Minor thrusts were found at the NE and SW of the study area with a parallel trend to the major thrust. The offset of strike-slip fault was seen with the fault plane in northwest - southwest trend and a left lateral sense of movement, while the offset strike slip fault trends approximately NNW – SSE with a right lateral sense of movement.

The main factors controlling the effective stress during folding and thrusting in the study area are northwest-southeast compressional stress, flexure folding, pressure build-up around the active faults, and fluid pressure changes.

Several folds styles were documented in the study area, they are; asymmetrical folds, chevron folds, tight folds and similar (class 3) folds, fault propagation folds and undulating cross folds.

The fractures have been indentified and grouped in to three sets, which are; longitudinal, transverse and oblique sets. The longitudinal (parallel to fold axis) set hosts the highest fracture density and is best developed in the area close to the fold hinge and varies with distance to the fold and has its highest density in thin-bedded limestone. Of the other two sets of fracture found in the area, the transverse set has lesser density compare to the longitudinal set.

This new understanding of fracture characteristics related to the structural styles in the Permian carbonates of Thailand is useful in creating better fracture network models.

6. Acknowledgements

I would like to express my gratitude to all those who gave me the possibility to complete this research project. I want to thank PTT Exploration and Production Ltd. for full scholarship to pursue this M.Sc. course. I would like to express my appreciation to Siam City Cement Company (SCCC) for giving me the excellent opportunities to study in the quarry and supported all information. I am heartily thankful to my supervisors Prof. John Keith Warren and Prof. Christopher K. Morley for their supervision, suggestions, recommendations and valuable ideas during this research project and throughout the course of study here in Chulalongkorn University. I am very grateful to Prof. Joseph Lambiase and Prof. Philip Rowell for their availability, support, and their valuable teaching and fresh ideas. Lastly, I am very thankful to my family, my colleagues and my friends for their encouragements and cheerfulness.

7. References

Hinthong, C., Chuaviroj, S., Kaewyana, V., Srisukh, S., and Pholprasit, C., 1981, Geology and Mineral Resources of the Map Sheet Changwat Phranakhon Sri Ayutthaya (ND 47-8): Department of the Mineral Resources, Geological Survey Report no.4 (in Thai).

Nelson, C. S., and Smith, A. M., 1996, Stable oxygen and carbon isotope compositional fields for skeletal and diagenetic components in New Zealand

Cenozoic nontropical carbonate sediments and limestones: a synthesis and review: New Zealand Journal of Geology and Geophysics, v. 39, p. 93-107.

Pothong, P., 1985, The geological and structure of Ratburi Group in a portion of the Eastern part of Changwat Saraburi, Central Thailand, Master thesis Chulalongkorn University.

Susanto, W., 2010, Diagenetic and isotopic evolution recorded in calcite cements in a large Indosinian Fault Zone in Permian platform interior carbonates, North Central Thailand: M Sc Research Report, Chulalongkorn University, 83 p.